Changes in Biomolecular Profile in a Single Nucleolus during Cell Fixation

ARTICLE *in* ANALYTICAL CHEMISTRY · SEPTEMBER 2014

Impact Factor: 5.64 · DOI: 10.1021/ac503172b · Source: PubMed

3 AUTHORS, INCLUDING:

Andrey N. Kuzmin
University at Buffalo, The State University of N…
90 PUBLICATIONS **1,260** CITATIONS
SEE PROFILE

Artem Pliss
University at Buffalo, The State University of N…
44 PUBLICATIONS **487** CITATIONS
SEE PROFILE

analytical chemistry

Article

pubs.acs.org/ac

Changes in Biomolecular Profile in a Single Nucleolus during Cell Fixation

Andrey N. Kuzmin,[†] Artem Pliss,[†] and Paras N. Prasad*

Institute for Lasers, Photonics and Biophotonics, Department of Chemistry, University at Buffalo, State University of New York, Buffalo, New York 14260-3000, United States

Supporting Information

ABSTRACT: Fixation of biological sample is an essential technique applied in order to "freeze" in time the intracellular molecular content. However, fixation induces changes of the cellular molecular structure, which mask physiological distribution of biomolecules and bias interpretation of results. Accurate, sensitive, and comprehensive characterization of changes in biomolecular composition, occurring during fixation, is crucial for proper analysis of experimental data. Here we apply biomolecular component analysis for Raman spectra measured in the same nucleoli of HeLa cells before and after fixation by either formaldehyde solution or by chilled ethanol. It is found that fixation in formaldehyde does not strongly affect the Raman spectra of nucleolar biomolecular components, but may significantly decrease the nucleolar RNA concentration. At the same time, ethanol fixation leads to a proportional increase (up to 40%) in concentrations of nucleolar proteins and RNA, most likely due to cell shrinkage occurring in the presence of coagulant fixative. Ethanol fixation also triggers changes in composition of nucleolar proteome, as indicated by an overall reduction of the α-helical structure of proteins and increase in the concentration of proteins containing the β-sheet conformation. We conclude that cross-linking fixation is a more appropriate protocol for mapping of proteins in situ. At the same time, ethanol fixation is preferential for studies of RNA-containing macromolecules. We supplemented our quantitative Raman spectroscopic measurements with mapping of the protein and lipid macromolecular groups in live and fixed cells using coherent anti-Stokes Raman scattering nonlinear optical imaging.

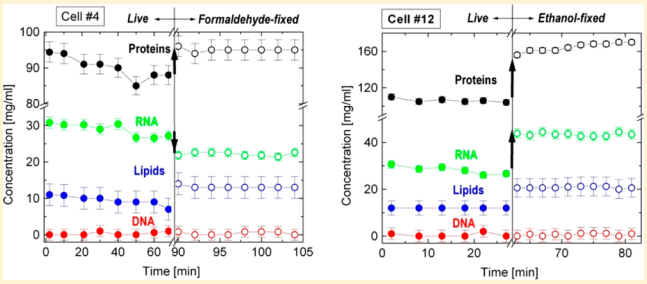

Methods used to research cellular molecular structure can be subdivided into two groups: those applied to live cells and those which investigate fixed cells. While the live cell studies have been generally recognized as more relevant and potentially more accurate in comparison with those performed on the fixed cells, cell fixation is required for many common bioassays including immunolabeling, electron microscopy, and IR spectroscopy. In order to perform an unambiguous analysis of the biological samples, the fixation procedure should preserve molecular structure of the live cell at the prefixation moment and prevent disintegration during the data collection. The common type of fixation is a chemical treatment of cells with either coagulants, such as alcohols, or cross-linking reagents, such as aldehydes. Despite being used for the same purpose, these two types of fixatives have very different impact on cellular biomolecular composition. Treatment with alcohols reduces the solubility of intracellular proteins and triggers their massive precipitation, whereas treatment with aldehydes creates cross-links between the soluble proteins, both protein and lipid constituents of membranes, cytoskeleton, genomic DNA, preventing decomposition of the cellular structure.[1] As a rule, the choice of fixative is dependent on the research tasks. For instance, in electron microscopy studies on cell and tissue morphology, preference is usually given to strong cross-linkers such as formaldehyde and glutaraldehyde, which ensure excellent preservation of biomolecular structures.[1] However, cross-links created by this class of fixatives mask various intracellular epitopes from recognition by antibodies, which may drastically reduce efficiency of immunostaining.[2] To avoid adverse effects of aldehyde fixation, the concentration and temperature of fixative as well as the time of fixation are strictly regulated. Furthermore, to facilitate immunolabeling of formaldehyde-fixed samples, many protocols utilize antigen-retrieval techniques, which involve heating of fixed samples and inevitably produce artifacts on the state of cellular structure.[3] Nevertheless, weak immunolabeling of formaldehyde-fixed samples is a major concern in immunohistochemical research. In comparison, cell fixation with alcohols allows for a much better preservation of antigens, but is notorious for producing structure artifacts and shrinking of biological samples.[4,5] Therefore, selection of the fixation protocols for each particular study involves meticulous screening of reports, where fixation was used for similar subject of research and extensive adjustments of methodology for each specific task.[1] It is worth noting that, in methods which interrogate the response

Received: August 23, 2014
Accepted: September 29, 2014
Published: September 29, 2014

   dx.doi.org/10.1021/ac503172b | Anal. Chem. 2014, 86, 10909−10916

of all macromolecules presented in the sample, such as optical spectroscopy, clear selection criteria of optimal fixation procedure are hard to define. It can lead to fixation-related artifacts that significantly impede the interpretation of results.[6]

Chemical fixatives are highly reactive molecules and produce significant aberrations in both distribution and biochemical properties of cellular molecules. Among the most prominent fixation effects on different biomolecules are protein cross-linkage, protein denaturation and coagulation, lipid solubilization, and reduction in DNA solubility and RNA quality.[7,8] Considering the impact of the fixation process on cellular structure, it is important to emphasize that neither precipitation nor cross-linking of cellular macromolecules occurs momentarily. For example, the formaldehyde almost instantaneously penetrates the cell, but reacts slowly; it requires ∼100 min to saturate half of the available cross-links sites on the cellular biomolecules and about 24 h to saturate them all.[9] The precipitation of macromolecules in the tissue with alcohols is not an instantaneous process either, known to take at least several minutes; moreover, in cells already fixed by alcohols a considerable diffusion of transmembrane proteins was reported.[10] At the same time molecular structure of a cell is extremely dynamic. Live cell bioimaging has revealed that significant changes in distribution of protein macromolecules, chromatin domains, and even large organelles may occur within only few seconds.[11−13] In this regard, dynamic changes of cellular structure may accompany the process of fixation, although these changes would not represent physiological processes and introduce artifacts of fixation. Hence, a comprehensive understanding of effects of fixation on the molecular organization of the cell is among the most fundamental problems in cell biology research. Unfortunately, there is a lack of established experimental methods which can support comprehensive analysis of molecular-level changes in cellular structures during the process of fixation. Conventional fluorescence labeling techniques are limited to detection of only several molecular species at a time. In contrast, biochemical techniques, which involve extraction of RNA and proteins, provide for detection of broad groups of cellular biomolecules, but inherently cannot interrogate any changes in subcellular distribution of biomolecules.

An efficient approach to study changes in biomolecular assemblies utilizes vibrational spectroscopies, including FT-IR[14] and Raman scattering technique.[15−18] For 2 decades Raman spectroscopy research has provided extensive data on the transformations of cellular structures during the fixation process.[6,19−25] These investigations mostly were performed using statistical approaches based on averaging of measurements over a number of different cells. For processing of multivariate Raman spectral data, acquired from biological samples, a principal component analysis (PCA) method is most frequently used.[26] A set of principal components, obtained in the process of PCA, shows variations in spectral bands assigned to specific chemical bonds and, therefore, gives a general idea about differences between the Raman spectra for a measured group of cells. Despite the progress obtained in previous studies, these multicell statistical approaches have significant drawbacks in identification of the impact which chemical fixatives have on cellular structure. Considerable cell-to-cell differences in biochemical composition are common even in genetically identical and synchronized populations of cells grown in the same culture.[27−29] Besides, earlier studies typically were performed in random sites of the cell nucleus or cytoplasm, regardless of distribution of specific organelles and structure function compartments of the cell nucleus. Meanwhile, distinct subcellular structures contain different sets of biomolecules and produce different Raman spectra.[30] Evidently, both the variability of cellular phenotypes and random selection of intracellular sites for spectral measurements may obscure changes in the Raman spectra produced solely by the fixation process and generate considerable ambiguity in data interpretation. Therefore, substantially more accurate and detailed data can be obtained by interrogation of specific organelles in single-cell assays, revealing the changes which take place during fixation.

This study is aimed at identification of fixation-related changes in specific cellular domains in single-cell assays. Changes to the biomolecular composition of nucleolus, the largest compartment in the cell nucleus, during fixation were studied. Biomolecular compositions were quantified using biomolecular component analysis (BCA) of Raman spectra obtained in nucleolus in situ of the same single cell before and after fixation. Studied transformations in the cellular structure were triggered by two commonly used coagulant and cross-linker fixatives, ethanol and formaldehyde, respectively. We found that these two fixation methods produce specific changes in the molecular structure of the nucleolus, which have to be carefully considered for design of experimental protocols and interpretation of data. Hence, our BCA approach can be a practical tool to observe fixation-induced artifacts and validate sample preparation procedures across a broad number of biomedical research fields.

MATERIALS AND METHODS

Preparation of Cell Samples. HeLa cells were grown in glass bottom dishes (Mattek), coated with an ∼10−20 μm collagen film. The Raman spectrum of collagen−water gel is shown to be extremely weak, reducing any strong contribution to the background.[31] Cells were cultured in Advanced DMEM (Invitrogen), supplemented with 2.5% fetal calf serum (Sigma), 1% glutamax, and 1% antibiotic antimycotic solution (Sigma) at 37 °C in a humidified atmosphere, containing 5% CO_2. For live cells assay, the cells were maintained in a Live-Cell (Pathology Devices) incubator chamber (37 °C at 80% humidity and 5% CO_2), mounted on the microscope stage. After finishing acquisition of Raman spectra in live cells, the cells were fixed in situ (while under the microscope) using either a 4% paraformaldehyde solution or chilled ethanol. For ethanol fixation, cells are placed at −20 °C for 10 min, while for paraformaldehyde fixation, the cells are kept at room temperature for 20 min. Prior to Raman spectra acquisition of fixed cells in PBS, cells are washed three times using the same PBS (pH 7.4) to remove any residual fixatives.

Raman Microscope. A confocal Raman microscope is used to acquire spectra from individual nucleoli. This set up consists of an inverted Nikon TE200 microscope, equipped with a He−Ne (632.8 nm, Coherent) laser and fiber-coupled MS3501i imaging monochromator/spectrograph (Solar TII) with a Hamamatsu S9974 CCD camera cooled down to −60 °C. This configuration enables measurements within the range of Raman shift of 600−3000 cm^{-1}. The spectral resolution for the fixed diffraction grating position (wavenumber interval of 1210 cm^{-1}) was ∼1.5 cm^{-1}. An excitation laser beam of ∼30 mW power was focused onto the sample in a spot of ∼0.8 μm, using a 100× NA = 1.3 Nikon oil-immersion objective lens. A 100 μm pinhole ensures for confocal acquisition of Raman signal,

dx.doi.org/10.1021/ac503172b | Anal. Chem. 2014, 86, 10909−10916

which corresponded to a confocality of ~1.8 μm (in WHDM) for the 632.8 nm laser wavelength. Detailed description of this instrumentation and tool calibration were described in our previous paper on cell cycle analysis.[30,32]

For better precision of measurements, Raman spectrum of a single nucleolus was acquired 5−10 times. The integration time for each spectral acquisition was 120 s for all experiments. To avoid any unwanted live cell cytotoxicity under prolonged laser irradiation, the interval between measurements in the same cell was above 2 min. Thus, spectroscopic studies performed in live cells did not produce any visible changes in cellular morphology (see Supporting Information Figure S1) and showed no cytotoxicity by standard viability tests. Measurements of fixed cells were performed after ~15 min following the washing procedure to obtain temperature equilibrium between the dish and the microscope stage, after which any drift along the objective axis (z-direction) was minimal.

CARS Imaging Microscope. Coherent anti-Stokes Raman scattering (CARS) imaging was performed with a Solar-TII CARS imaging system (Supporting Information Figure S2), as described previously.[30,33] The images were collected during sequential scans corresponding to the CARS resonances of proteins at ~2910 cm^{-1} and of lipids at ~2850 cm^{-1}, and nonresonance background at ~2970 cm^{-1}, with the time interval between scans ~3 min. Then nonresonance background was subtracted from the images of the proteins and lipids.

Processing of Raman Spectra. In the first step, the raw Raman spectra of the live cell nucleolus (Supporting Information Figure S3) and corresponding background (Raman signal at the closest location out of the cell at the same depth) were acquired. Then the background spectra for the same nucleolus were averaged (Supporting Information Figure S4) and modeled by fitting to the five background components (Supporting Information Figure S5). Fitted background curves (Supporting Information Figure S4) were then used for background subtraction. We used modeled background profiles instead of measured ones to avoid the effect of small uncontrollable fluctuations during background measurements on further spectra analysis. After background subtraction, the procedure of Savitzky−Golay smoothing (2nd polynom order, 13 points smoothing frame) and baseline correction were applied to the Raman spectra, which then were used for further biomolecular component analysis (Supporting Information Figure S6). The measurements, performed on fixed cells where biomolecular concentration changes due to live cell cycle were "frozen", demonstrated that experimental error of Raman spectra did not exceed 2−5% within the Raman shift range of 700−1700 cm^{-1} (Supporting Information Figures S7 and S8).

Biomolecular Component Analysis. For assessment of intranucleolar macromolecular information, the biomolecular component analysis (BCA)[32] was applied to preprocessed Raman spectra. This method is based on an accurate spectral fit of a model spectrum, the linear summation of the weighted spectra of the basic components (linear combination modeling (LCM)[34−37]), into a preprocessed Raman spectrum of the nucleoli. The spectral weights (coefficients) are considered as the specific contributions of the basic spectra into the resulting spectrum and relate directly to the concentrations of basic macromolecules. In our case, LCM of the acquired Raman spectra was utilized for experimental evaluation of the local biomolecular composition in HeLa cells' nucleoli by generating a model spectrum through a linear summation of weighted Raman spectra of the basic classes of organic biomolecules, which make the largest contribution to the nucleolar Raman spectrum (DNA, RNA, proteins, lipids).[32] In mathematical terms, it means to obtain a numerical value of the fractional fit contribution (weight, C_i) of each component, i, to the Raman spectrum of measured nucleolar domain (r_{total}): $r_{total} = C_1r_1 + C_2r_2 + C_3r_3 + C_4r_4$, where r_i is the Raman spectrum of the ith-component. The LCM algorithm was developed using a Matlab environment; it contains several cycles of fitting the weighted model with the measured spectrum, including the separation of DNA and RNA contributions. A more detailed description of BCA used in this study can be found in our previous publication.[32] For the initial step of BCA, we used protein component (r_1), obtained from our previous studies of HeLa cell culture[32] corresponding to 100 mg/mL of bovine serum albumin ($C_1 = 1$) equivalent concentration. Then the protein spectra were defined more accurately during further steps of BCA. Preprocessed Raman spectra of extracted DNA, RNA, and lipid droplets from HeLa cells, calibrated to 20 mg/mL of calf thymus DNA, *Saccharomyces cerevisiae* RNA, and bovine heart lipid extract accordingly, were used as the reference spectra for the DNA, RNA, and lipids components (r_i, i = 2, 3, 4 with $C_i = 1$, i = 2, 3, 4).

RESULTS AND DISCUSSION

Effect of Fixation on Cellular Morphology and Large-Scale Macromolecular Structure of the Cell. In the preliminary experiments, we estimated the influence of fixation by formaldehyde and ethanol on the morphology and biomolecular structure of the cell. We observed that formaldehyde preserves the morphology of cells in conditions close to that of live cells, while ethanol fixation results in characteristic transformations of cell morphology. At high resolution, cell shrinkage and emergence of fibrillar aggregates in the cell interior apparently due to precipitation of proteins in ethanol-fixed cells could be identified (Supporting Information Figure S1).

We advanced morphological analysis by selective label-free mapping of protein and lipid macromolecules in the same cell before and after fixation, using CARS nonlinear imaging. CARS imaging employs stimulated Raman scattering processes, characterized by amplified output signal, allowing for rapid image acquisitions. We observed that in live cells proteins occupy the entire cellular volume with local enrichment in the nucleoli. Signal corresponding to lipid resonance is associated mostly with cytoplasm, membranes, and in many cells bright lipid droplets were also seen (Supporting Information Figure S9). We found that the formaldehyde fixation did not considerably change the signal intensity and distribution for both intracellular proteins and lipids biomolecules. At the same time, a comparison of the CARS images, obtained before and after fixation by ethanol, shows marked changes in distribution of proteins and lipids. The precipitation of biomolecules leads to emergence of large intracellular granules, visible both in the protein and lipid CARS images. The fixation-related distortions also include an increase into the protein signal intensity in the nucleolus and perinuclear region. Local increases in the signal intensity were seen for the cytoplasmic lipids as well, mostly in the area surrounding the nucleus. Hence, the analysis of the distribution of proteins and lipids before and after fixation shows that ethanol fixation produces nonuniform changes in the cellular structure, most likely due to the differences in

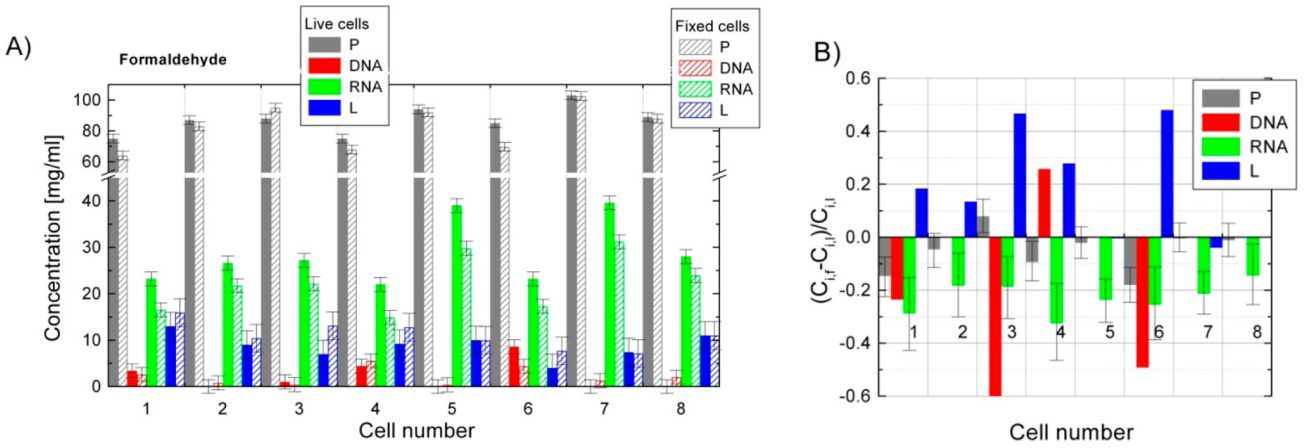

Figure 1. (A) Concentrations of proteins (P), DNA, RNA, and lipids (L) obtained by BCA for one nucleolus per cell before (solid bars) and after (patterned bars) the formaldehyde fixation. (B) Relative differences between concentrations of biomolecular components in live ($C_{i,l}$) and fixed ($C_{i,f}$) nucleoli. Error bars represent standard error (SE), see Supporting Information Figure S8. Error values for DNA and lipids are comparable to that of corresponding relative concentrations and are not shown in panel B.

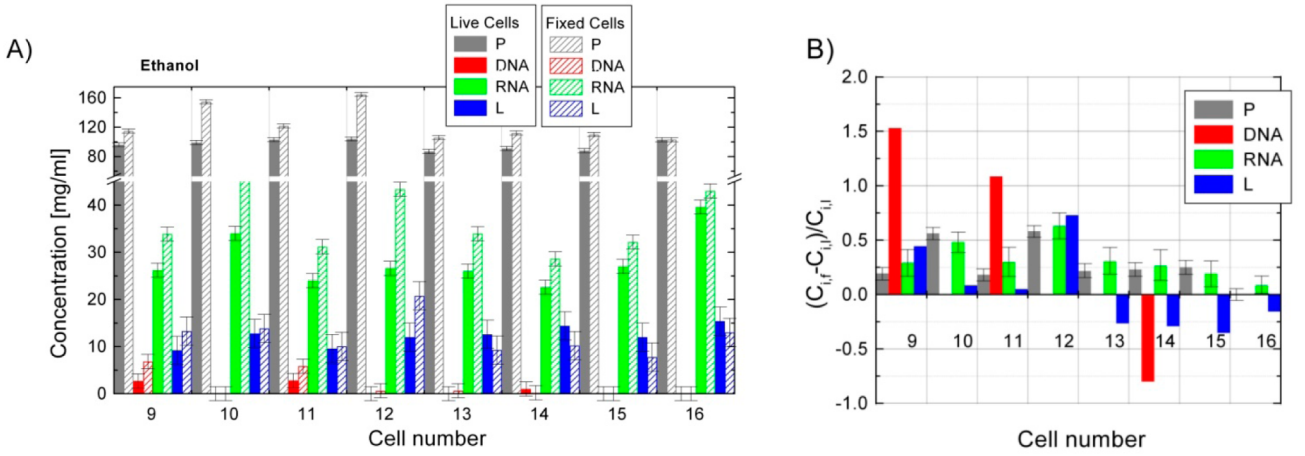

Figure 2. (A) Concentrations of proteins (P), DNA, RNA, and lipids (L) obtained by BCA for one nucleolus per cell before (solid bars) and after (patterned bars) the ethanol fixation. (B) Relative differences between concentrations of biomolecular components in live ($C_{i,l}$) and fixed ($C_{i,f}$) nucleoli. Error bars represent SE, see Supporting Information Figure S8. Error values for DNA and lipids are comparable to that of corresponding relative concentrations and are not shown in panel B.

interactions of various molecular constituencies of the cell with ethanol.

Effect of Fixation on Biomolecular Composition of Nucleolus. A quantitative analysis on the influence of fixation process on the cellular macromolecular structure was studied in two experimental groups, each containing eight HeLa cells. Potential changes of molecular structure in the process of fixation were studied on the specific example of nucleolus. The nucleolus is a convenient model for Raman microspectroscopy as it can be unambiguously distinguished in the cell nucleus by transmission light imaging. Furthermore, this nuclear organelle is typically several micrometers in diameter, which is several times larger than the size of the beam waist of the probe laser. At the same time, data analysis points to averaging of a signal from substantial volume of nucleolus, which facilitates reproducibility of spectra measurements. In our earlier study we described that spectra acquired across the center of the same nucleolus are essentially similar, regardless heterogeneous molecular content of the nucleolar interior.[32]

Despite the reports on the gradual course of a fixation procedure,[38] it is generally assumed that all biochemical process taking place in live cells are immediately stopped when fixatives are added, and distribution of biomolecules is well-preserved corresponding to that at the moment prior to fixation.[22] A single-cell Raman assay provides for direct monitoring of cellular structure and quantitative identification of potential changes in process of fixation.

In our study we identified mitotic cells and tracked them into the interphase. All the measurements were performed 3−4 h after cell division to minimize any potential variations in the content of nucleolus related to the cell-cycle progression. For spectral measurements, cells with a representative morphology and large nucleoli with dimensions exceeding the confocal parameter of the device (Supporting Information Figure S1) were selected in order to ensure that the contribution of the extranucleolar region to the collected Raman signal is not substantial. The spectra were acquired in the time lapse mode for ∼30−60 min for a single nucleolus per cell. The BCA technique was used to identify concentrations of RNA, proteins, DNA, and lipids in the nucleoli as described in the Materials and Methods section. Remarkably, the BCA results unravel pronounced transformations of molecular composition

dx.doi.org/10.1021/ac503172b | Anal. Chem. 2014, 86, 10909−10916

Table 1. Result of t Test Series ($p < 0.05$) for Paired (Live/Fixed) Sets of Nucleolar Biomolecular Components Obtained by BCA

	proteins	significantly different	DNA	significantly different	RNA	significantly different	lipids	significantly different
live/fixed by formaldehyde	$t = 1.73769$	N	$t = 0.00181$	N	$t = 10.1359$	Y	$t = -2.6828$	Y
	$p = 0.12583$		$p = 0.99861$		$p = 1.95713 \times 10^{-5}$		$p = 0.03141$	
live/fixed by ethanol	$t = -3.7157$	Y	$t = -1.57575$	N	$t = -4.97007$	Y	$t = -0.0185$	N
	$p = 0.0075$		$p = 0.15909$		$p = 0.00162$		$p = 0.98575$	

of the nucleolus in live cultured cells. We observed that concentrations of RNA and proteins fluctuate in time. Within 5−10 min intervals between measurements, RNA and protein concentrations were changing upwards of 5−30% and 5−10%, respectively (Supporting Information Figures S10 and S11). These drifts likely reflect the changing intensity of RNA synthesis in nucleolus and are subject of our separate investigation.

After 30−60 min, the cells being monitored were fixed directly onto the microscopy stage, rinsed with buffer, and Raman monitoring of the same nucleolus was continued for another 20−30 min (Supporting Information Figures S10 and S11).

BCA indicates a pronounced transformation in the molecular composition of the same nucleolus after fixation process. By comparing the biomolecular composition of the nucleolus derived from the last acquisition of the time-lapse measurements in the live cell and that of just fixed cell, we found significant differences specific for each type of fixative. The impact of fixation on nucleolar content is shown in Figures 1 and 2, where the parameter $(C_{i,f} - C_{i,l})/C_{i,l}$ represents the relative difference between concentrations of the corresponding ith-component of the live (index l) and the fixed (index f) nucleolus.

Formaldehyde fixation results in a considerable reduction of the RNA content (∼20−30%) in nucleoli of all studied cells. At the same time, changes in the concentration of proteins were less pronounced. We observed in five of the eight studied cells, a reduction of proteins concentration from 5% to 18%, whereas in one of the studied cells we measured an ∼8% increase. We also found a tendency of an increase in lipid concentrations in nucleoli, upon the formaldehyde fixation, although in some cells this was not observed (Figure 2A).

In contrast to formaldehyde, fixation with ethanol leads to an increase of both protein and RNA nucleolar concentrations from ∼10% to 60%. In individual cells, this increase was nearly proportional for both molecular components (Supporting Information Figure S12). However, the concentrations of nucleolar lipids changed either up or down after the ethanol fixation, with no clear trend detected. Our data show no correlation between the changes of lipids and two dominant types of nucleolar molecules (RNA and proteins) in both types of fixation. Monitoring the fixed cells in time shows only negligible changes of the macromolecular profiles, which indicates that each fixative ensured preservation of the structural integrity of the nucleoli. Probable mechanism responsible for the increase in concentration of biomolecules in the nucleoli of the ethanol-fixed cells could be precipitation of protein macromolecules and dehydration, accompanied by cell shrinkage as a consequence of coagulative properties of ethanol.[7] In the process of the ethanol fixation, the volume of nucleolus decreased (Supporting Information Figure S1B), which suggests that nucleolar macromolecules became accumulated in a smaller volume, leading to an increase in the density of nucleolus. The proportional growth in both RNA and protein concentrations fits this scenario well.

In contrast to ethanol, formaldehyde produces no visible changes in the size of the nucleolus. This fixative is known to react with side chains of proteins to form cross-links, thus immobilizing proteins and stabilizing cellular structure.[7] Consistent with the fact that proteins are the primary target of formaldehyde reaction, we observed relatively low changes in the protein concentration. At the same time, a decrease to the amount of nucleolar RNA can be caused by partial degradation of nucleic acid in the presence of formaldehyde.[8] Also, cross-link formation can affect weak intermolecular forces between RNA and protein constituents of ribonucleoprotein complexes, resulting in some loss of RNA at early stages of fixation.

To verify the trend of the biomolecular concentration changes caused by fixation process, we performed eight t tests with two paired groups, each containing nucleolar biomolecular concentrations of the same molecular type (proteins, DNA, RNA, lipids) from live (group 1) and fixed (group 2) cells of the same cell set. Changes of RNA content in the case of formaldehyde fixation and those of proteins/RNA contents in the case of ethanol fixation are significantly different (see Table 1).

This finding is also consistent with classical immunohistochemical studies comparing the utility of protocols involving either cross-linking by formaldehyde or precipitation by methanol for labeling of nucleolar RNA. Methanol fixation resulted in a strong signal from the nucleolar RNA, whereas formaldehyde-fixed cells had nearly absent nucleolar RNA signal.[39] The authors concluded that the higher RNA signal was due to superior accessibility of nucleolar epitopes in ethanol-fixed cells as compared to the nucleoli where molecules were cross-linked by formaldehyde. Our data show that a higher concentration of RNA in the nucleoli of ethanol-fixed cells can also contribute to a stronger signal.

The largest relative differences were found for lipids and DNA concentrations for both types of fixation (Figures 1 and 2). However, in these cases, concentrations of biomolecules were close to the measurement confidence level and the analysis of relative changes is a cumbersome task.

Analysis of Protein Component Difference Profiles. The impact of fixatives on the proteins populating the nucleolus is not well-studied. The nucleolar proteome accommodates up to three thousands of different proteins with different sizes, amino-acid composition, spatial conformation, charge, solubility, and other physicochemical properties.[40] To complicate matters, many proteins remain after fixation structurally intact and at the same location, while other proteins, even when using strong cross-linking fixatives, may be differentially extracted and redistributed in the cellular volume.[41−43] In addition, both coagulation or cross-linking fixatives may have an impact on vibrational frequencies of different chemical bonds and

therefore change Raman spectra,[44] compromising further analysis. In this regard, the studies of the difference profiles of normalized Raman spectra of protein components corresponding to the same nucleolus before and after fixation allow for identification of changes in the nucleolar proteome during the fixation process. Detailed methodology for obtaining the protein component during BCA was described in our earlier studies on Raman spectral assessment of the nucleolus of HeLa cells.[32] Our method assumes that the nucleolus is composed mostly of proteins, nucleic acids, and lipid macromolecules. When DNA, RNA, and lipid model components are subtracted from the averaged Raman spectrum, the remaining spectral profile is assigned to the "proteins" model component for further analysis. The "proteins" profile includes contribution of all nucleolar proteins, although small organic and inorganic molecules may contribute as well. Also, one should consider that this residual spectral profile for a fixed nucleolus could be deformed by potential differences of spectra of nucleic acids and lipids emerging from the fixation. Using this method we computed BCA protein components for each individual cell before and after fixation (Supporting Information Figure S13). Difference profiles between the averaged protein component spectra of live and fixed cells, overlapped with typical nucleolus proteins component, are presented in Figure 3. The signal intensity of the difference profile for the ethanol-fixed cells is considerably higher than the error margin, rising up to 50% of the corresponding spectrum intensity (red curve, Figure 3a). We observed an increase in the intensity of spectral bands centered at 1242 and 1670 cm^{-1} and a decrease in the intensity of spectral bands centered at 723, 1120, 1337, 1414, and 1650 cm^{-1}. Generally, all these peaks can be potentially generated due to changes of Raman spectra of all major biomolecules (proteins, DNA, RNA, and lipids) during the fixation process.

Proteins. The positive peaks at 1242 and 1670 cm^{-1} and the negative peaks at 1337 and 1650 cm^{-1} in the difference spectrum indicate a reduction in the α-helical structure[44,45] and an increase in the proportion of β-sheet conformation[46] in the composition of the nucleolar proteome, respectively. The negative spectral band centered at 723 cm^{-1} is assigned to methionine/tyrosine and C−C−C deformations, while the 1120 cm^{-1} band is attributed to tryptophan and C−C/C−N stretching.

DNA and Minor Types of Cellular Biomolecules. The contribution of DNA and minor types of biomolecules is apparently insignificant (within the limits of experimental error) due to initially low concentrations of these types of molecules inside the nucleolar domain.

Lipids. The peaks of the Raman spectrum obtained for HeLa cellular lipids are not correlated with the peaks of difference spectrum (red curve, Figure 3a), and therefore, contribution of lipids to difference Raman profile is not expected.

RNA. The prominent peaks of difference profile at ∼722, ∼1242, and at ∼1337 cm^{-1} could be associated with unaccounted changes of RNA Raman bands assigned to adenine in the first and third cases, and uracil/cytosine/adenine in the second case.[47] In general, the following phenomena could produce changes of intensity of Raman bands of RNA molecule: (i) hypochromism (hyperchromism), where an increase (decrease) in length of RNA with defined helical structure is leading to a decrease (increase) in the intensity of the affected Raman band, and (ii) changes in spatial conformation, which are usually accompanied as well by changes in hydrogen bonding. If we assume that during the ethanol fixation the RNA molecule is partially disintegrated to smaller chains of nucleotides, then the appearance of a positive peak at ∼1242 cm^{-1}, which for RNA is hypochromic, and negative peak at ∼722 cm^{-1}, which for RNA is hyperchromic (red curve, Figure 3a) should be accompanied by a strong positive hypochromic peak at 980 cm^{-1};[47] that is not the case. Moreover, the most prominent RNA intensity sensitive marker for changing of conformation, the band centered at ∼814 cm^{-1},[47,48] is located within the limits of standard error. In this regard, the RNA component is unlikely responsible for Raman spectrum changes mentioned above.

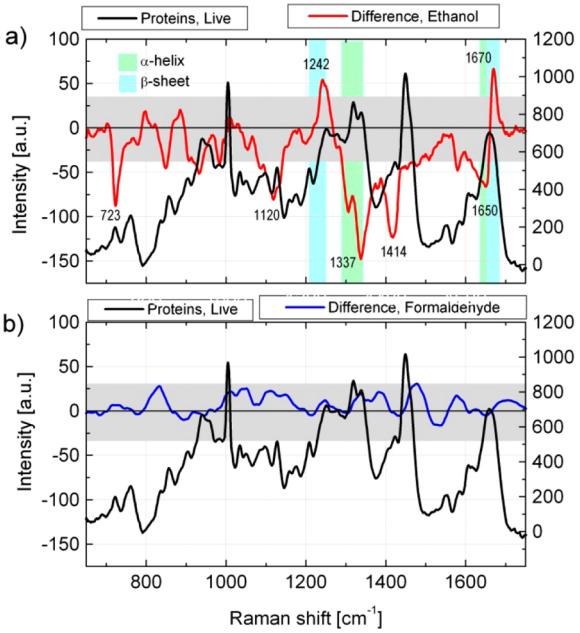

Figure 3. Representative "nucleolar proteins" component of live cell (black color, right *Y*-axis) overlapped with difference profiles between proteins Raman spectra of fixed and live cells, averaged through the corresponding cell group. The blue curve corresponds to the formaldehyde fixation group, red to ethanol fixation, both associated with the left *Y*-axis. Before averaging, all spectra were normalized to the 1004 cm^{-1} protein line. The wavenumber regions, where deviations after fixation were found, are marked by corresponding numbers. The gray band represents the intensity region of experimental error for difference profiles (left *Y*-axis). Color columns confine amide I and amide III spectral bands associated with protein conformations. The assignments for these regions were taken from refs 44 and 45: 723 cm^{-1}, methionine, tyrosine, C−C−C deformations; 1120 cm^{-1}, tryptophan, C−C and C−N stretching; 1242 cm^{-1}, amide III (β-strand); 1337 cm^{-1}, amide III (α-helix); 1414 cm^{-1}, C−H deformation; 1650 cm^{-1}, amide I (α-helix); 1670 cm^{-1}, amide I (β-strand).

Consequently, the changes in the nucleolar protein component spectrum, observed after ethanol fixation, appeared most likely due to reduction of proteins with α-helical structure and an increase in the portion of proteins containing the β-sheet conformation.

In contrast to results observed for ethanol fixation, the signal intensity of difference profile for cells fixed by formaldehyde (Figure 3b) is very close to the margins of standard error (∼3−5% depending on Raman shift, Supporting Information Figure S8). This means that the Raman spectra of the nucleoli following formaldehyde fixation are qualitatively similar to those of live cells; at least these changes are beyond the sensitivity of our experimental setup. Hence, although form-

dx.doi.org/10.1021/ac503172b | Anal. Chem. 2014, 86, 10909−10916

aldehyde fixation has been reported to produce considerable changes in the distribution of many proteins,[41−43] our data indicates that this fixation protocol preserves the spectral signature of nucleolar proteome and other nucleolar macromolecules well.

The three-dimensional (3D) conformation of proteins is a decisive factor in the process of molecular recognition. In particular, immune recognition is generally thought of as a "lock-and-key" described by Fisher[49] where the complex molecular structure of the epitope is matched by the antigen-binding fragments of antibody. In this regard, conformation changes of proteins during the ethanol fixation may severely impact the efficiency of immunolabeling. Our data suggest that formaldehyde fixation may promote more effective labeling of proteins. At the same time, many nuclear proteins are present in the cell nucleus in complexes with RNA, known as ribonucleoproteins. The observed reduction of RNA content in the process of formaldehyde fixation (Figure 1) may cause structural transformation of the epitope and, therefore, result in a loss of the ability of immune recognition.

CONCLUSION

A quantitative understanding of how the molecular structure of the cell may be transformed in the process of fixation is of utmost importance for the interpretation of experimental data analysis of biomedical assays as well as for further advancement of research methodology. At the same time, fixation is known to induce changes in the structure of biological samples. At different resolution levels these changes include (i) structural deformation and degradation of some cellular biomolecules, (ii) redistribution of biomolecules, and (iii) large-scale alterations to morphology of organelles and cells. Earlier studies have identified numerous fixation-related changes in cellular structure by generalizing data obtained on large cellular populations. However, considerable variations in biomolecular composition of different cellular organelles as well as of individual cells could limit efficiency of traditional cell-population averaging assays. In our study, we employed a combination of two specific approaches to overcome this obstacle: first, monitoring of fixation effect was performed on a single cell and to the same organelle using the Raman spectroscopy technique; second, changes in local macromolecular environment were characterized quantitatively through BCA-generated biomolecular profiles. This combinative approach enabled us to reveal specific changes introduced by commonly used fixatives and to disclose a number of advantages and disadvantages of specific fixation protocols. Besides superior preservation of the cell morphology, fixation in formaldehyde provides for a good preservation of proteins in nucleolus. Despite cross-linking, we found no significant changes in the concentration and conformation of the nucleolar proteins. This finding is consistent with earlier cell fixation studies by Raman spectroscopy. Meade et al.[22] concluded that formalin fixation preserves a cellular Raman spectrum similar to that of the live cell. At the same time, this method of fixation may significantly reduce the nucleolar RNA concentration. Most likely, this is one of the fixation effects, which was masked by using statistical signal averaging approaches adopted by earlier studies. In contrast to formaldehyde, ethanol fixation leads to proportional increases in the concentrations (up to 40%) of nucleolar proteins and RNA, apparently due to cell shrinkage. Another consequence of ethanol fixation is a significant reduction of proteins with α-helical structure and an increase in the portion of proteins containing the β-sheet conformation in the composition of nucleolar proteome.

Our results suggest that fixation with coagulative fixatives, such as ethanol, may be preferable to improve detection of RNA and potentially RNA binding proteins. Also data analysis points out to substantial cell-to-cell variability in the changes of nucleolar content during either type of fixation. The protoplasm of each cell is inherently variable in concentrations of various biomolecules, intracellular pH, viscosity, and other physical−chemical properties. Hence, fixatives may cause different types of macromolecular redistribution during the fixation and this process cannot be generalized for the entire cellular population.

Variability found in our data emphasizes the importance of the single-cell experimental approach. Finally, we conclude that BCA is likely the most proper tool when dealing with Raman data of single-cell assay. Although PCA is useful for highlighting spectrum peculiarities in cellular ensembles, it is not efficient for molecular composition analysis of cellular domains, where significant cell-to-cell concentration variations of basic macromolecules occur. As follows from the result of PCA applied to the same set of cells (see the Supporting Information), this technique significantly yields to BCA in confidence and completeness of obtained data. All of these findings contribute to comprehensive interpretation of experimental data obtained in the cells after fixation.

ASSOCIATED CONTENT

Supporting Information

Transmission and CARS images of measured cells, raw and processed Raman spectra, background and standard error curves for cell no. 3, BCA results for time-lapse measurements, individual BCA proteins components, and PCA analysis. This material is available free of charge via the Internet at http://pubs.acs.org.

AUTHOR INFORMATION

Corresponding Author

*Phone: 716-645-4148. E-mail: pnprasad@buffalo.edu.

Author Contributions

†A.N.K. and A.P. contributed equally to this work.

Notes

The authors declare no competing financial interest.

ACKNOWLEDGMENTS

This work was supported by AFOSR Grant No. FA9550-12-1-0226.

REFERENCES

(1) Griffiths, G.; Burke, B.; Lucocq, J. *Fine Structure Immunocytochemistry*; Springer-Verlag: Berlin, New York, 1993; p xxi.

(2) Werner, M.; Chott, A.; Fabiano, A.; Battifora, H. *Am. J. Surg. Pathol.* **2000**, *24*, 1016−1019.

(3) Hunt, N. C. A.; Attanoos, R.; Jasani, B. *J. Clin. Pathol.* **1996**, *49*, 767−770.

(4) Benezra, J.; Johnson, D. A.; Rossi, J.; Cook, N.; Wu, A. *J. Histochem. Cytochem.* **1991**, *39*, 351−354.

(5) Gedrange, T.; Mai, R.; Mack, F.; Zietek, M.; Borsos, G.; Vegh, A.; Spassov, A.; Gredes, T. *J. Physiol. Pharmacol.* **2008**, *59*, 87−94.

(6) Mariani, M. M.; Lampen, P.; Popp, J.; Wood, B. R.; Deckert, V. *Analyst* **2009**, *134*, 1154−1161.

(7) *Theory and Practice of Histological Techniques*, 6th ed.; Bancroft, J. D., Gamble, M., Eds.; Churchill Livingstone/Elsevier: Philadelphia, PA, 2008; pp 1 online resource (xv, 725 p).
(8) Kok, L. P.; Boon, M. E. *Microwaves for the Art of Microscopy*; Coulomb Press: Leyden, Netherlands, 2003.
(9) Helander, K. G. *Biotech. Histochem.* **1994**, *69*, 177−179.
(10) Tanaka, K. A. K.; Suzuki, K. G. N.; Shirai, Y. M.; Shibutani, S. T.; Miyahara, M. S. H.; Tsuboi, H.; Yahara, M.; Yoshimura, A.; Mayor, S.; Fujiwara, T. K.; Kusumi, A. *Nat. Methods* **2010**, *7*, 865−866.
(11) Chan, D. C. *Cell* **2006**, *125*, 1241−1252.
(12) Pliss, A.; Malyavantham, K. S.; Bhattacharya, S.; Berezney, R. *J. Cell. Physiol.* **2013**, *228*, 609−616.
(13) Phair, R. D.; Misteli, T. *Nature* **2000**, *404*, 604−609.
(14) Whelan, D. R.; Bambery, K. R.; Puskar, L.; McNaughton, D.; Wood, B. R. *Analyst* **2013**, *138*, 3891−3899.
(15) Puppels, G. J.; Demul, F. F. M.; Otto, C.; Greve, J.; Robertnicoud, M.; Arndtjovin, D. J.; Jovin, T. M. *Nature* **1990**, *347*, 301−303.
(16) Schulze, H. G.; Konorov, S. O.; Piret, J. M.; Blades, M. W.; Turner, R. F. B. *Analyst* **2013**, *138*, 3416−3423.
(17) Palonpon, A. F.; Sodeoka, M.; Fujita, K. *Curr. Opin. Chem. Biol.* **2013**, *17*, 708−715.
(18) Wei, L.; Yu, Y.; Shen, Y. H.; Wang, M. C.; Min, W. *Proc. Natl. Acad. Sci. U.S.A.* **2013**, *110*, 11226−11231.
(19) Shim, M. G.; Wilson, B. C. *Photochem. Photobiol.* **1996**, *63*, 662−671.
(20) Faolain, E. O.; Hunter, M. B.; Byrne, J. M.; Kelehan, P.; Lambkin, H. A.; Byrne, H. J.; Lyng, F. M. *J. Histochem. Cytochem.* **2005**, *53*, 121−129.
(21) Chan, J. W.; Taylor, D. S.; Thompson, D. L. *Biopolymers* **2009**, *91*, 132−139.
(22) Meade, A. D.; Clarke, C.; Draux, F.; Sockalingum, G. D.; Manfait, M.; Lyng, F. M.; Byrne, H. J. *Anal. Bioanal. Chem.* **2010**, *396*, 1781−1791.
(23) Konorov, S. O.; Schulze, H. G.; Caron, N. J.; Piret, J. M.; Blades, M. W.; Turner, R. F. B. *J. Raman Spectrosc.* **2011**, *42*, 576−579.
(24) Mazur, A. I.; Marcsisin, E. J.; Bird, B.; Miljkovic, M.; Diem, M. *Anal. Chem.* **2012**, *84*, 1259−1266.
(25) Mazur, A. I.; Marcsisin, E. J.; Bird, B.; Miljkovic, M.; Diem, M. *Anal. Chem.* **2012**, *84*, 8265−8271.
(26) Kallaway, C.; Almond, L. M.; Barr, H.; Wood, J.; Hutchings, J.; Kendall, C.; Stone, N. *Photodiagn. Photodyn. Ther.* **2013**, *10*, 207−219.
(27) Eldar, A.; Elowitz, M. B. *Nature* **2010**, *467*, 167−173.
(28) Chalancon, G.; Ravarani, C. N. J.; Balaji, S.; Martinez-Arias, A.; Aravind, L.; Jothi, R.; Babu, M. M. *Trends Genet.* **2012**, *28*, 221−232.
(29) Kaern, M.; Elston, T. C.; Blake, W. J.; Collins, J. J. *Nat. Rev. Genet.* **2005**, *6*, 451−464.
(30) Pliss, A.; Kuzmin, A. N.; Kachynski, A. V.; Prasad, P. N. *Biophys. J.* **2010**, *99*, 3483−3491.
(31) Bonnier, F.; Meade, A. D.; Merzha, S.; Knief, P.; Bhattacharya, K.; Lyng, F. M.; Byrne, H. J. *Analyst* **2010**, *135*, 1697−1703.
(32) Kuzmin, A. N.; Pliss, A.; Kachynski, A. V. *J. Raman Spectrosc.* **2013**, *44*, 198−204.
(33) Pliss, A.; Kuzmin, A. N.; Kachynski, A. V.; Prasad, P. N. *Proc. Natl. Acad. Sci. U.S.A.* **2010**, *107*, 12771−12776.
(34) Buschman, H. P.; Deinum, G.; Motz, J. T.; Fitzmaurice, M.; Kramer, J. R.; van der Laarse, A.; Bruschke, A. V.; Feld, M. S. *Cardiovasc. Pathol.* **2001**, *10*, 69−82.
(35) Shafer-Peltier, K. E.; Haka, A. S.; Fitzmaurice, M.; Crowe, J.; Myles, J.; Dasari, R. R.; Feld, M. S. *J. Raman Spectrosc.* **2002**, *33*, 552−563.
(36) Short, K. W.; Carpenter, S.; Freyer, J. P.; Mourant, J. R. *Biophys. J.* **2005**, *88*, 4274−4288.
(37) Swain, R. J.; Kemp, S. J.; Goldstraw, P.; Tetley, T. D.; Steyens, M. M. *Biophys. J.* **2010**, *98*, 1703−1711.
(38) Fox, C. H.; Johnson, F. B.; Whiting, J.; Roller, P. P. *J. Histochem. Cytochem.* **1985**, *33*, 845−853.
(39) Koberna, K.; Stanek, D.; Malinsky, J.; Ctrnacta, V.; Cermanova, S.; Novotna, J.; Kopsky, V.; Raska, I. *Acta Histochem.* **2000**, *102*, 15−20.
(40) Andersen, J. S.; Lam, Y. W.; Leung, A. K.; Ong, S. E.; Lyon, C. E.; Lamond, A. I.; Mann, M. *Nature* **2005**, *433*, 77−83.
(41) Melan, M. A.; Sluder, G. *J. Cell Sci.* **1992**, *101* (Pt 4), 731−743.
(42) Guillot, P. V.; Xie, S. Q.; Hollinshead, M.; Pombo, A. *Exp. Cell Res.* **2004**, *295*, 460−468.
(43) Schnell, U.; Dijk, F.; Sjollema, K. A.; Giepmans, B. N. G. *Nat. Methods* **2012**, *9*, 152−158.
(44) Maiti, N. C.; Apetri, M. M.; Zagorski, M. G.; Carey, P. R.; Anderson, V. E. *J. Am. Chem. Soc.* **2004**, *126*, 2399−2408.
(45) Nemecek, D.; Stepanek, J.; Thomas, G. J., Jr. *Current Protocols in Protein Science*; Coligan, J. E., Dunn, B. M., Ploegh, H. L., Speicher, D. W., Wingfield, P. T., Eds.; Wiley: Hoboken, NJ, 2013; Chapter 17, Unit17 18.
(46) Tsuboi, M.; Suzuki, M.; Overman, S. A.; Thomas, G. J. *Biochemistry* **2000**, *39*, 2677−2684.
(47) Hobro, A. J.; Standley, D. M.; Ahmad, S.; Smith, N. I. *Phys. Chem. Chem. Phys.* **2013**, *15*, 13199−13208.
(48) Thomas, G. J.; Hartman, K. A. *Biochim. Biophys. Acta* **1973**, *312*, 311−322.
(49) Fischer, E. *Ber. Dtsch. Chem. Ges.* **1894**, *27*, 2985−2993.